Supporting Information for:

Ultrafast Spectroscopy of [Mn(CO)$_3$] Complexes: Tuning the Kinetics of Light-Driven CO Release and Solvent Binding

Wade C. Henke,[†] Christopher J. Otolski,[†,‡] William N. G. Moore,[#] Christopher G. Elles, and James D. Blakemore**

Department of Chemistry, University of Kansas
1567 Irving Hill Road, Lawrence, KS 66045

* To whom correspondence should be addressed: E-mail: blakemore@ku.edu; phone: +1 (785) 864-3019 (JDB). E-mail: elles@ku.edu; phone: +1 (785) 864-1922 (CGE).

[†] These authors contributed equally to this work.
[‡] Current address: Chemical Sciences and Engineering Division, Argonne National Laboratory, Lemont, Illinois 60439
[#] Current address: Department of Chemistry, University of California at Irvine, Irvine, California 92617

Contents

NMR Spectra

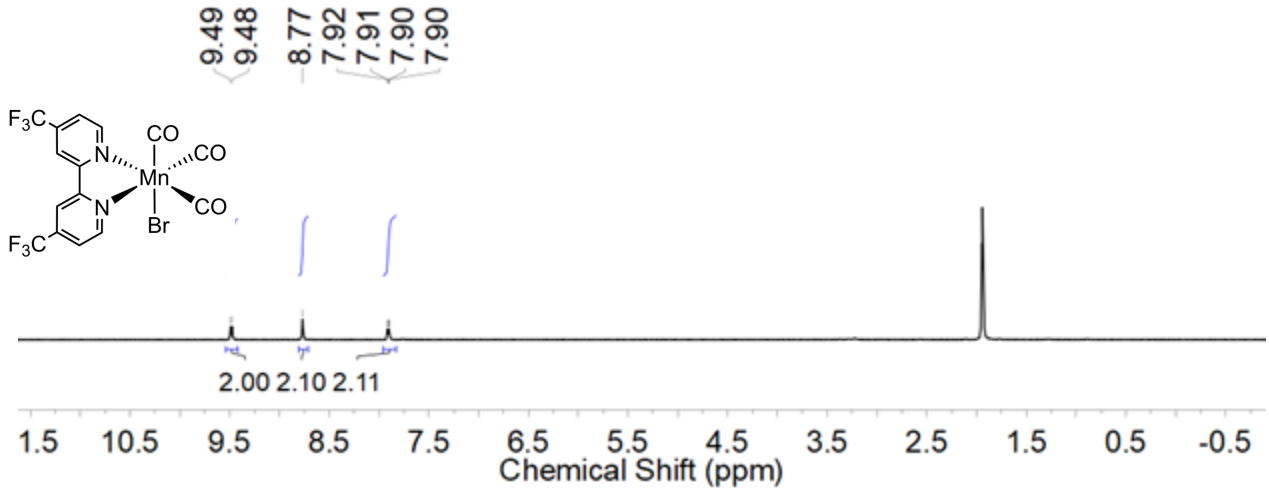

Figure S1: ^{1}H-NMR spectrum (400 MHz, CD3CN) of **3.**

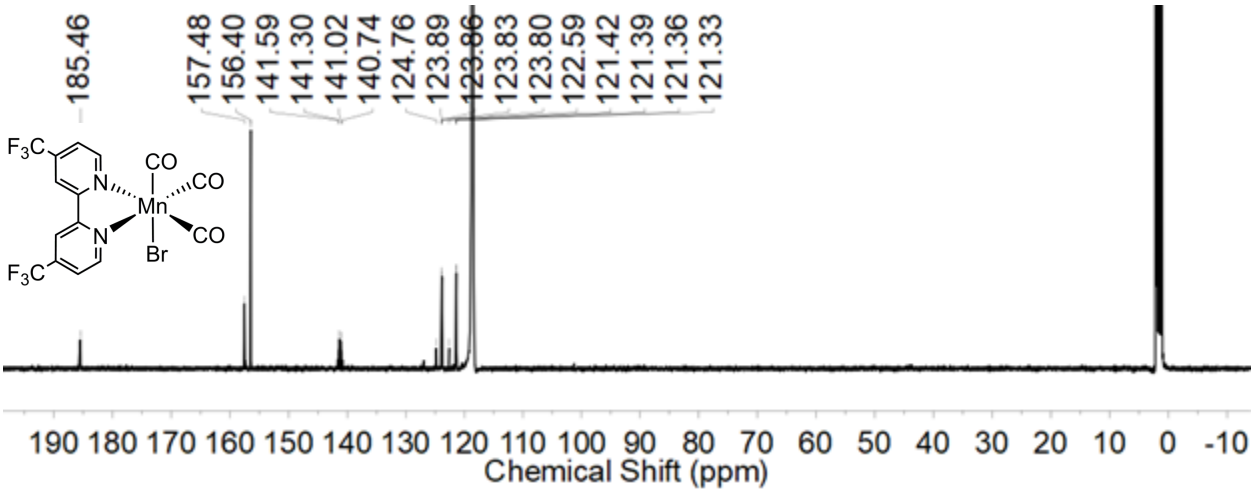

Figure S2: ^{13}C{^{1}H} NMR spectrum (126 MHz, CD_3CN) of **3.**

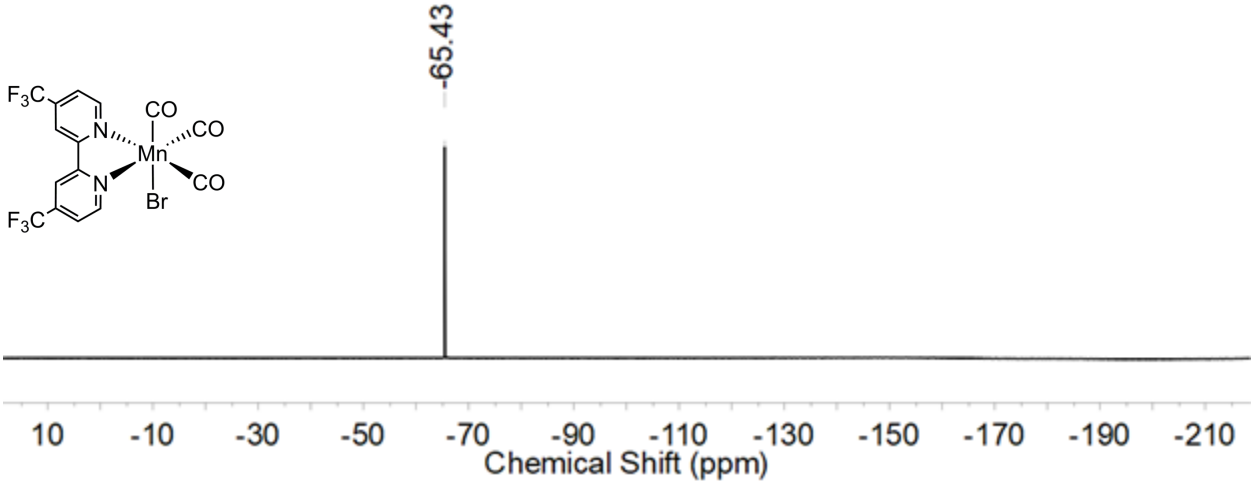

Figure S3: ^{19}F-NMR spectrum (376 MHz, CD_3CN) of **3.**

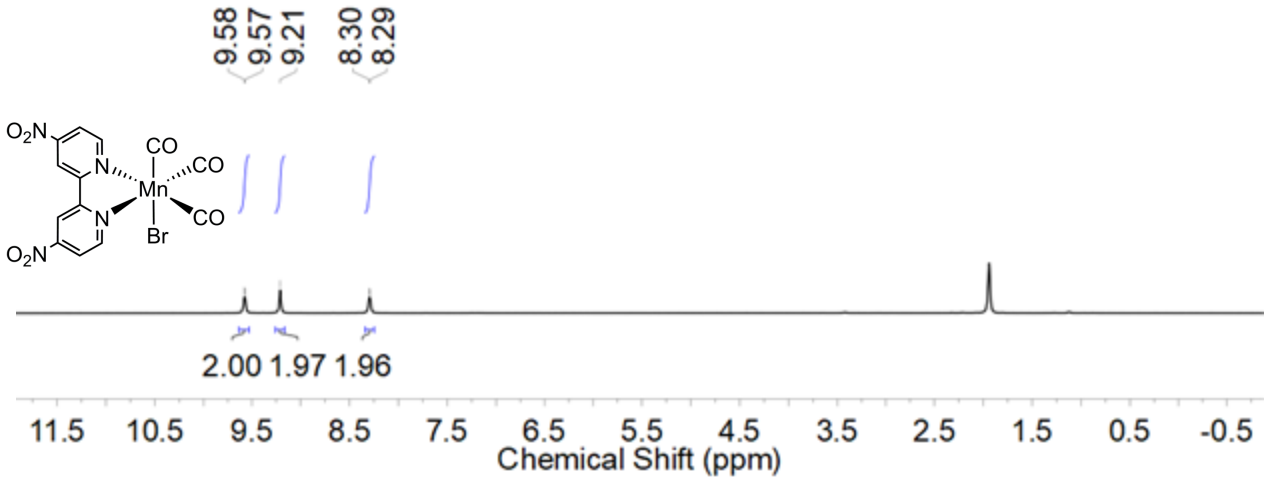

Figure S4: ^{1}H-NMR spectrum (400 MHz, CD3CN) of **4.**

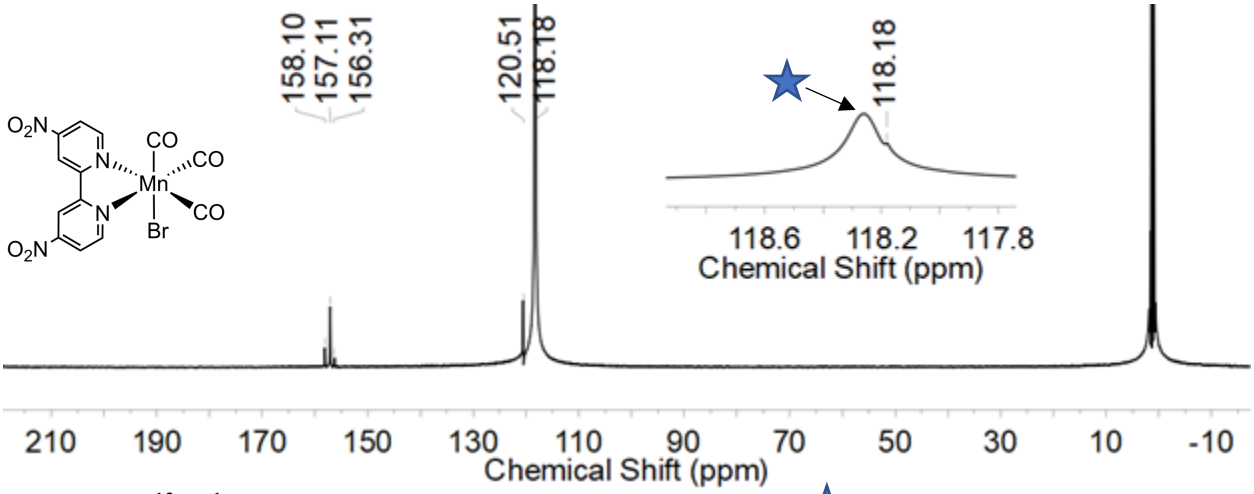

Figure S5: ^{13}C{^{1}H} NMR spectrum (126 MHz, CD_3CN) of **4**; ★ indicates the solvent residual.

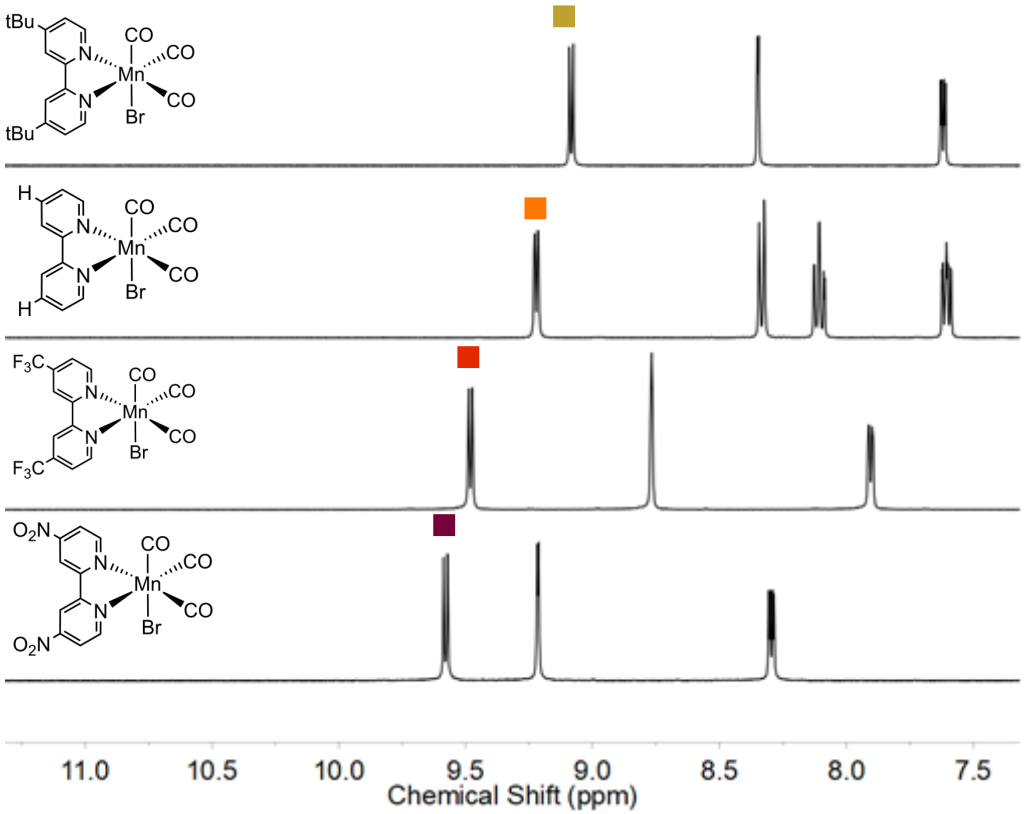

Figure S6: Stacked ^{1}H-NMR spectra (400 MHz, CD3CN) of **1**, **2**, **3**, and **4** in the aromatic region.

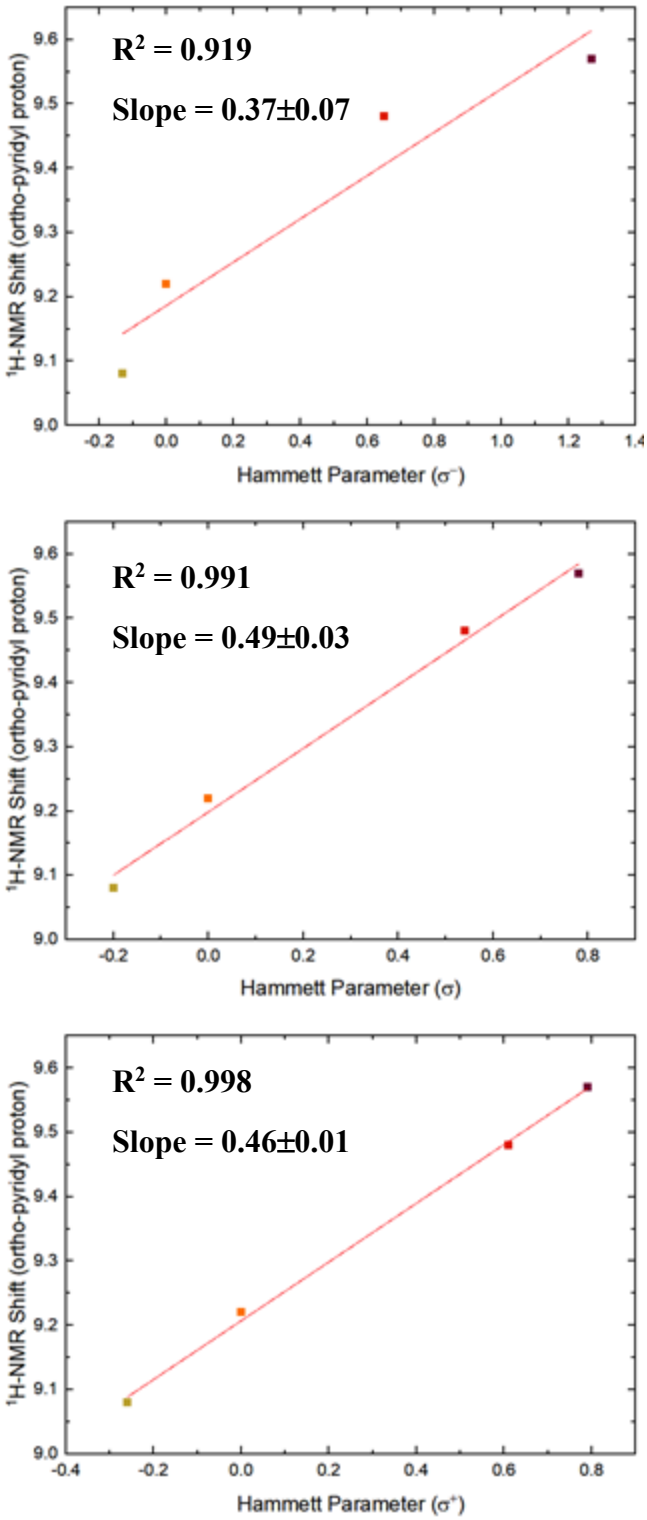

Figure S7: Hammett analyses showing the correlation between the ^{1}H-NMR shift of the ortho-pyridyl proton as a function of the various Hammett Parameters σ^{-} (top), σ (middle), and σ^{+} (bottom). The best fit is found when the data is plotted as a function of the σ^{+} Hammett Parameter.

IR Data

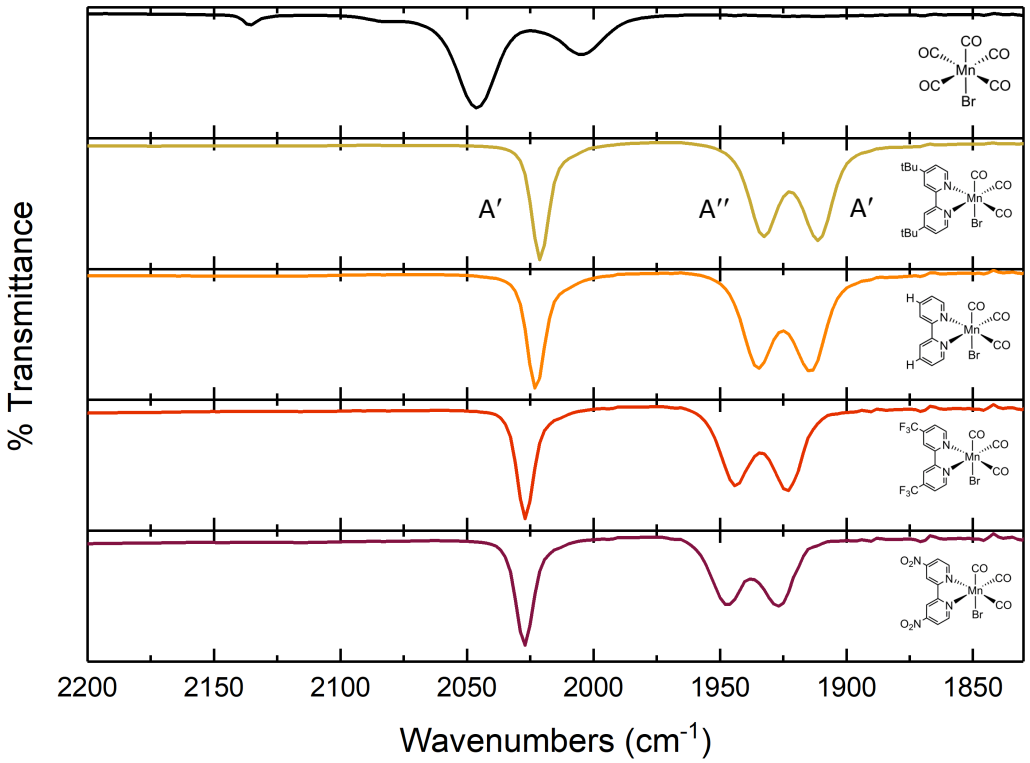

Figure S8: IR spectra of $Mn(CO)_5Br$, **1**, **2**, **3**, and **4** in THF in the CO stretching region. For a C_s symmetric molecule three CO stretches ($\Gamma_{CO} = 2A'+A''$) is expected, and the expected three features are observed for **1**, **2**, **3**, and **4**.

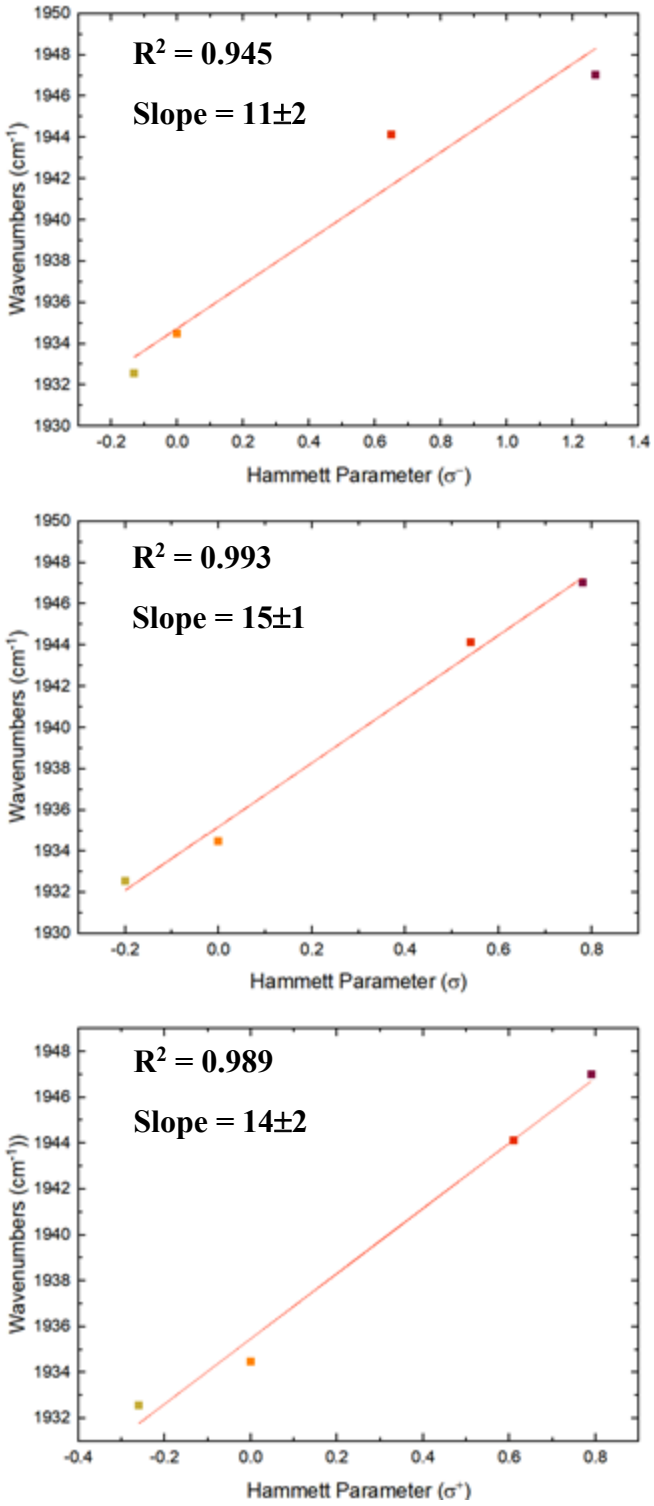

Figure S9: Hammett Analyses showing the correlation between the wavenumbers of the CO stretch as a function of the various Hammett Parameters σ^- (top), σ (middle), and σ^+ (bottom). The best fit is found when the data is plotted as a function of the σ Hammett Parameter.

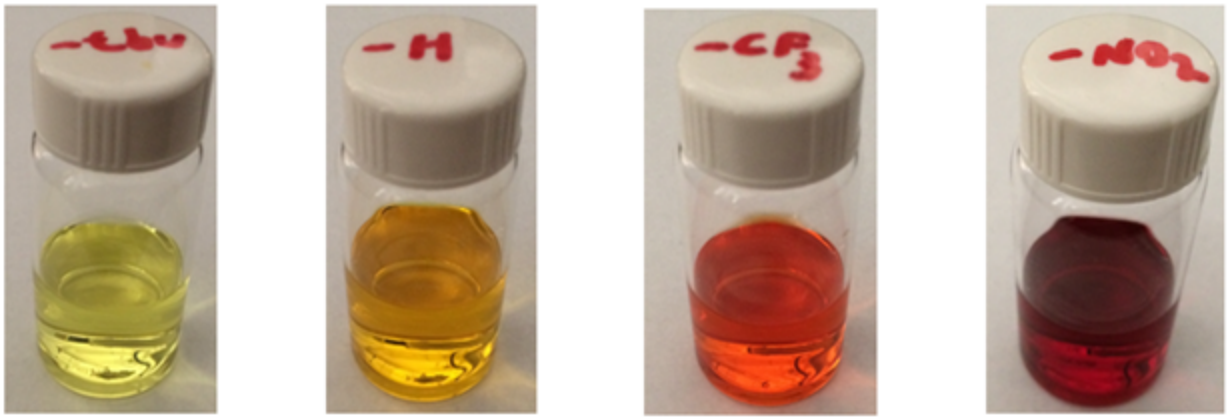

Figure S10: Prepared solutions of the [Mn(CO)3Br(^{R}bpy)] complexes in MeCN.

UV-Vis, Transient Absorption, and Gas Chromatography Data

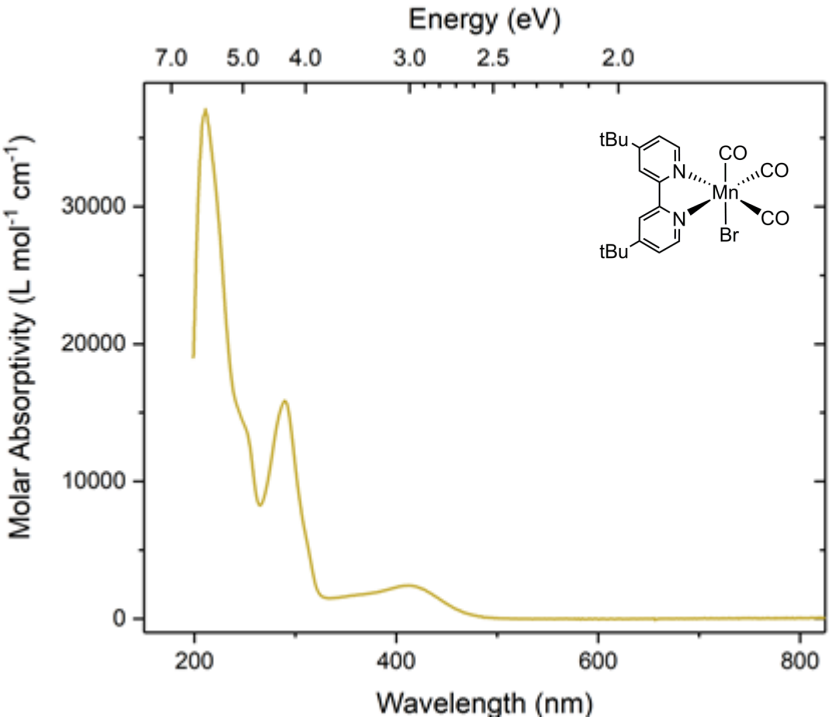

Figure S11: Electronic absorption spectrum of **1** in MeCN. The smaller tic marks are used to illustrate 0.1 eV increments.

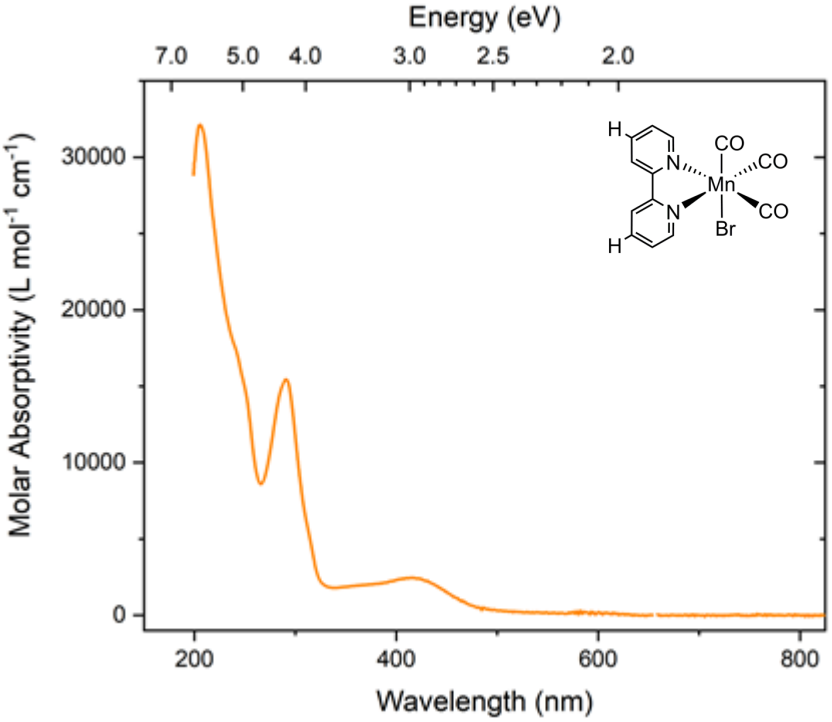

Figure S12: Electronic absorption spectrum of **2** in MeCN. The smaller tic marks are used to illustrate 0.1 eV increments.

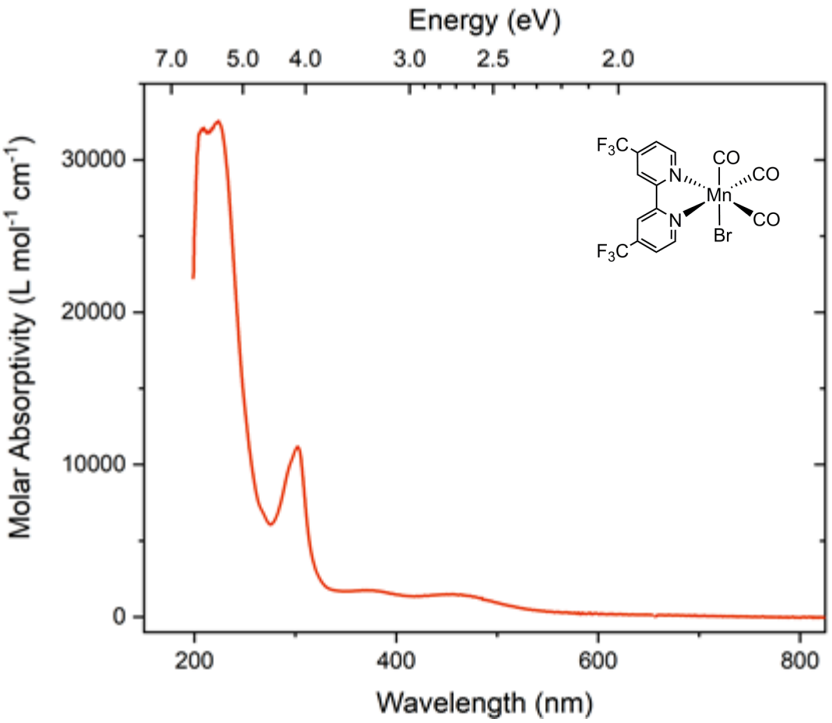

Figure S13: Electronic absorption spectrum of **3** in MeCN. The smaller tic marks are used to illustrate 0.1 eV increments.

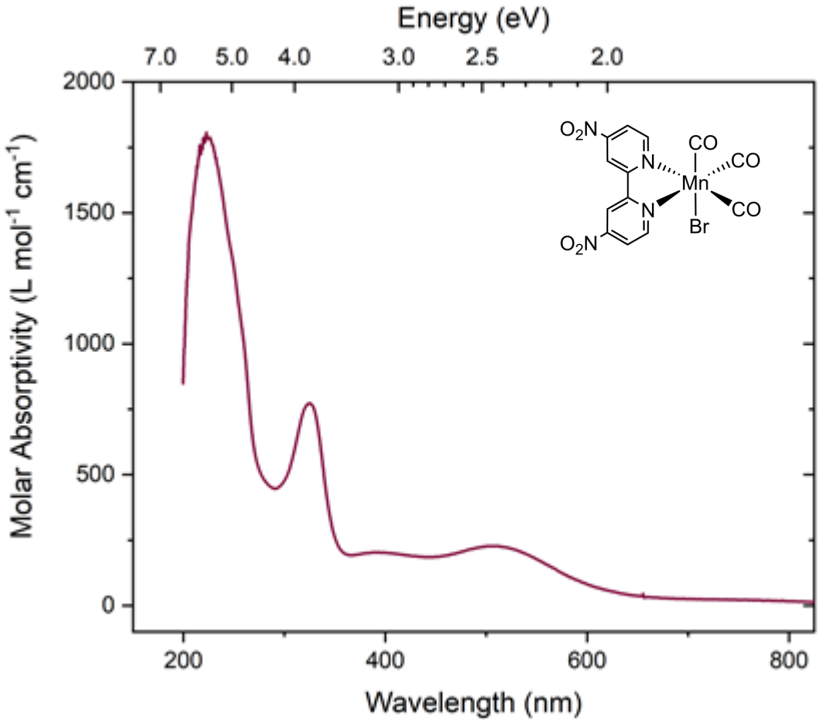

Figure S14: Electronic absorption spectrum of **4** in MeCN. The smaller tic marks are used to illustrate 0.1 eV increments.

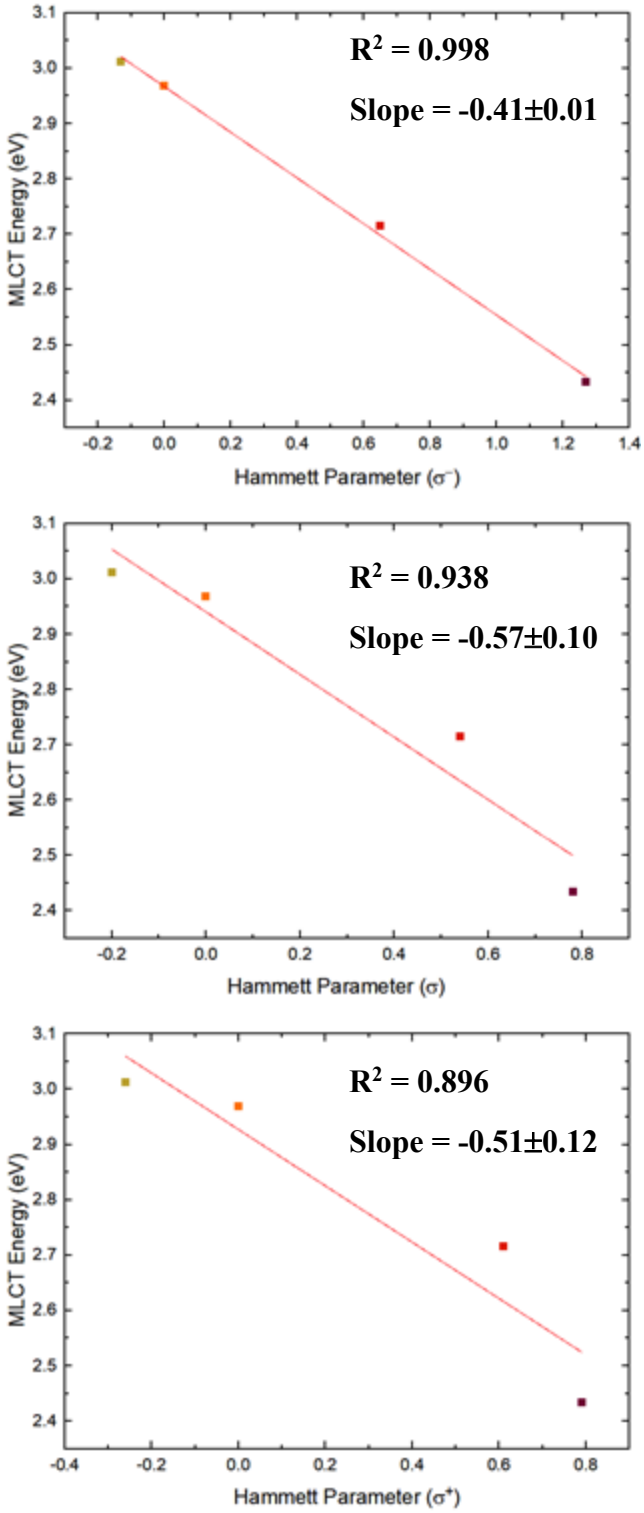

Figure S15: Hammett Analyses showing the correlation between the MLCT energy band as a function of the various Hammett Parameters σ^- (top), σ (middle), and σ^+ (bottom). The best fit is found when the data is plotted as a function of the σ^- Hammett Parameter.

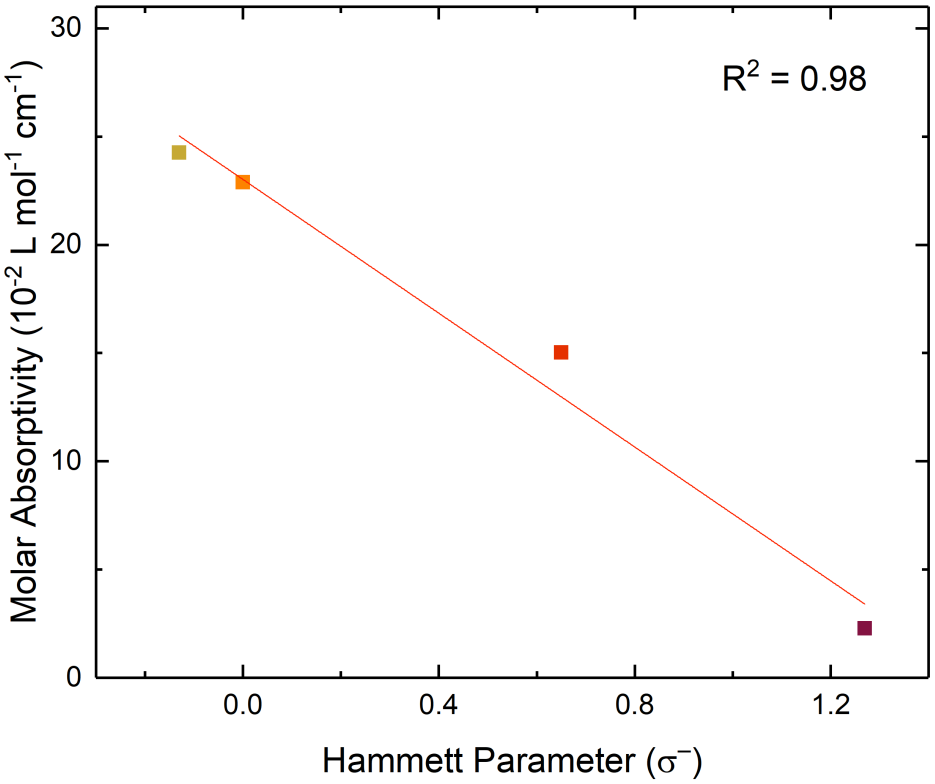

Figure S16: Molar absorptivity as a function of the Hammett Parameter for complexes **1-4**. The low molar absorptivity for **4** may be due to significant d-d character, but the trend established here may indicate that the absorption retains MLCT character.

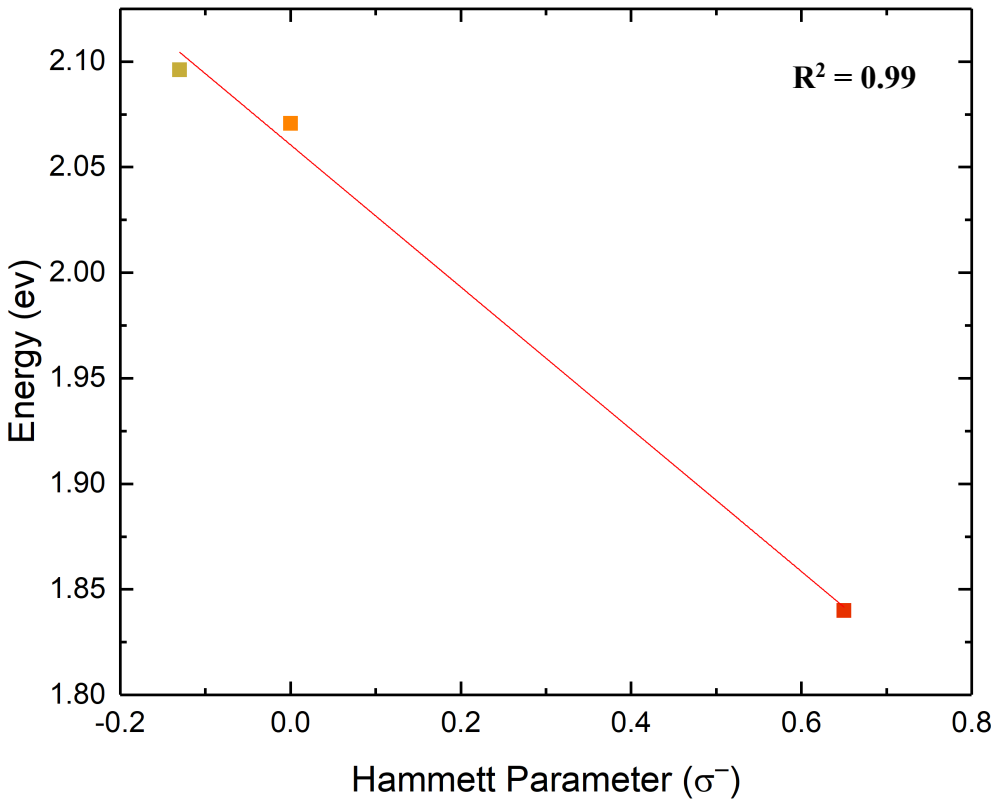

Figure S17: Hammett analysis of the excited state absorption maxima at longer wavelengths for the analogous solvent coordinated species arising from CO loss from **1**, **2**, and **3** correlating the lowest-energy band (an apparently shifted MLCT feature) as a function of Hammett Parameter (σ^-).

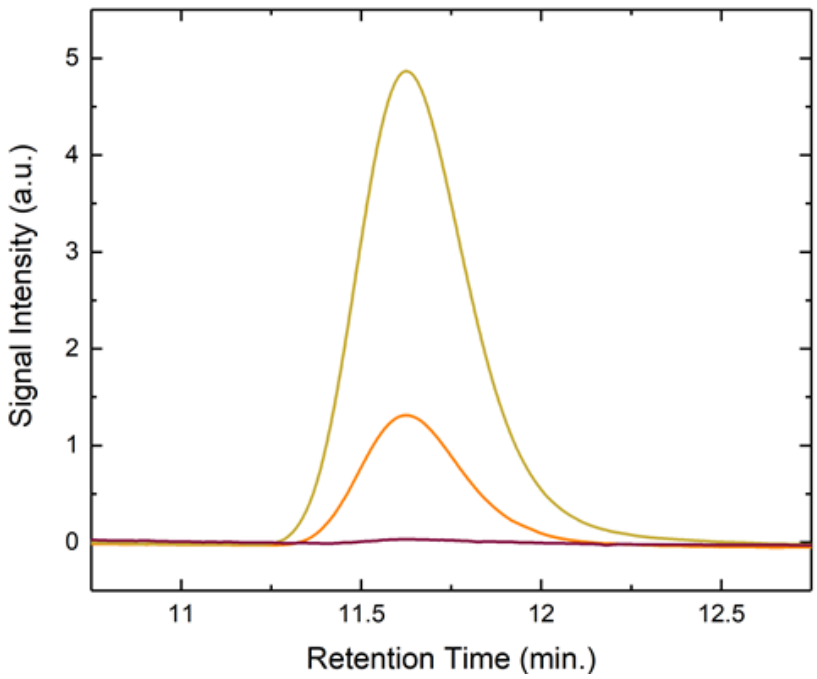

Figure S18: Monitoring of CO release by gas chromatography from photolysis of **1** (yellow; photolyzed at 420 nm), **2** (orange; photolyzed at 420 nm), and **4** (purple; photolyzed at 510 nm), for two hours. Signal intensity is normalized by solution concentration of complex in MeCN.

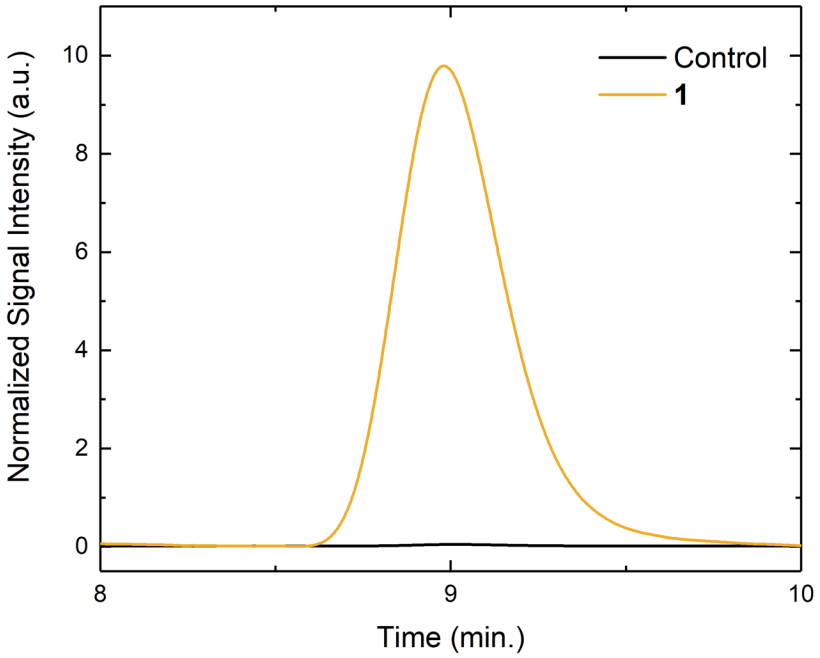

Figure S19: CO release measured by gas chromatography for photolysis of a 5-mL solution of **1** (dark yellow line; photolyzed at 420 nm) for 2 hours and comparison with a related control experiment with a 5-mL sample of **1** stored in the dark over a period of 10 hours. Signal intensity for yield of CO by gas chromatography is normalized by solution concentration of complex **1** in MeCN, headspace volume, and experiment time.

Calculation of the apparent rates of CO loss show that the compound releases CO at a substantially faster rate upon irradiation (1.2 mol CO (mol Mn)$^{-1}$ day^{-1}) versus in the dark by slower thermal reactivity (0.003 mol CO (mol Mn)$^{-1}$ day^{-1}). [**1**] in each experiment was 10^{-3} M. Lamp characteristics are as described in the Experimental Section.

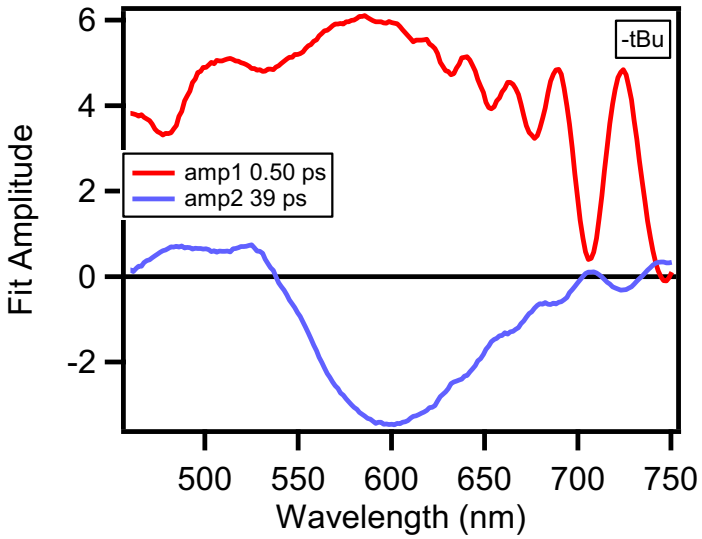

Figure S20: Fit of the decay associated spectrum for **1** to extract kinetic data.

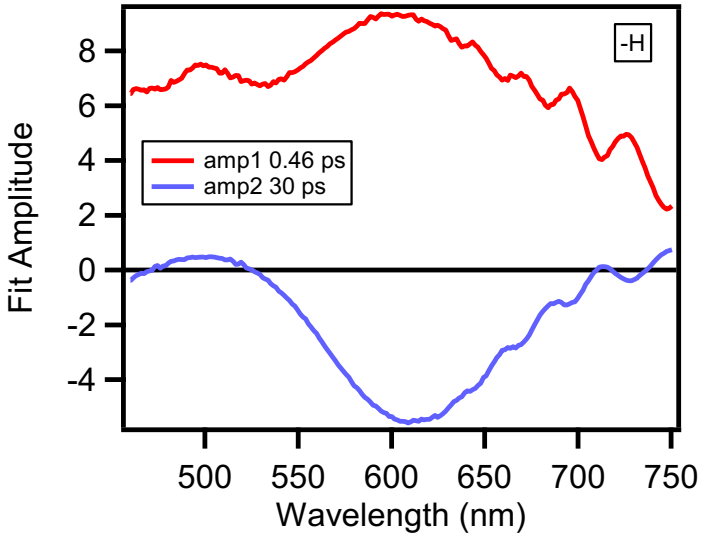

Figure S21: Fit of the decay associated spectrum for **2** to extract kinetic data.

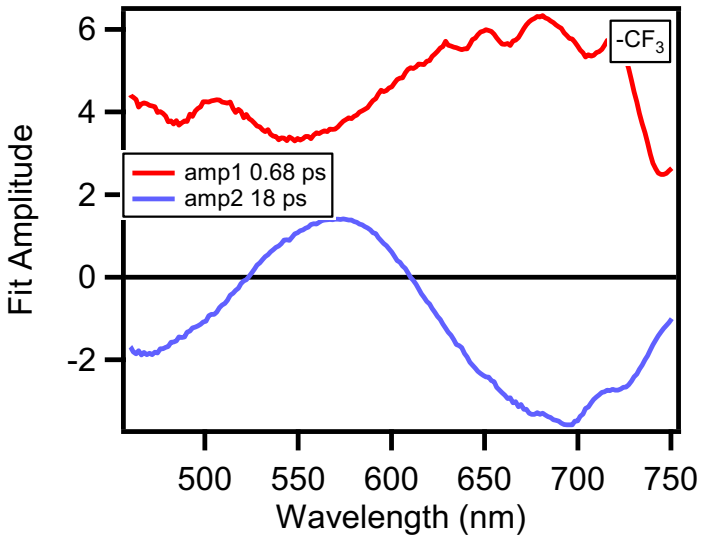

Figure S22: Fit of the decay associated spectrum for **3** to extract kinetic data.

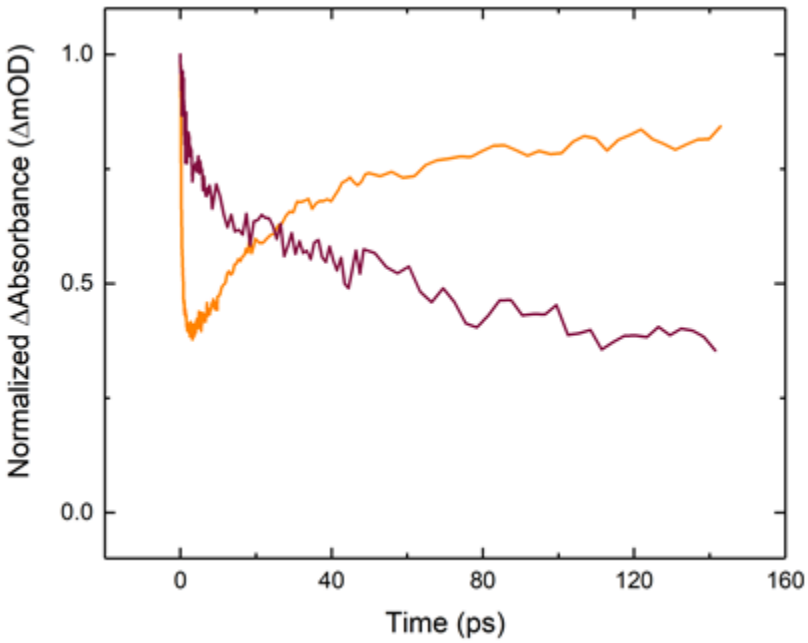

Figure S23: Comparison of the normalized ΔAbsorbance as a function of time for compounds **2** (monitored at 600nm—orange line) and **4** (monitored at 580nm—purple line); Complex **2** undergoes solvent coordination, while complex **4** undergoes vibrational cooling and forms an apparently long lived MLCT state.

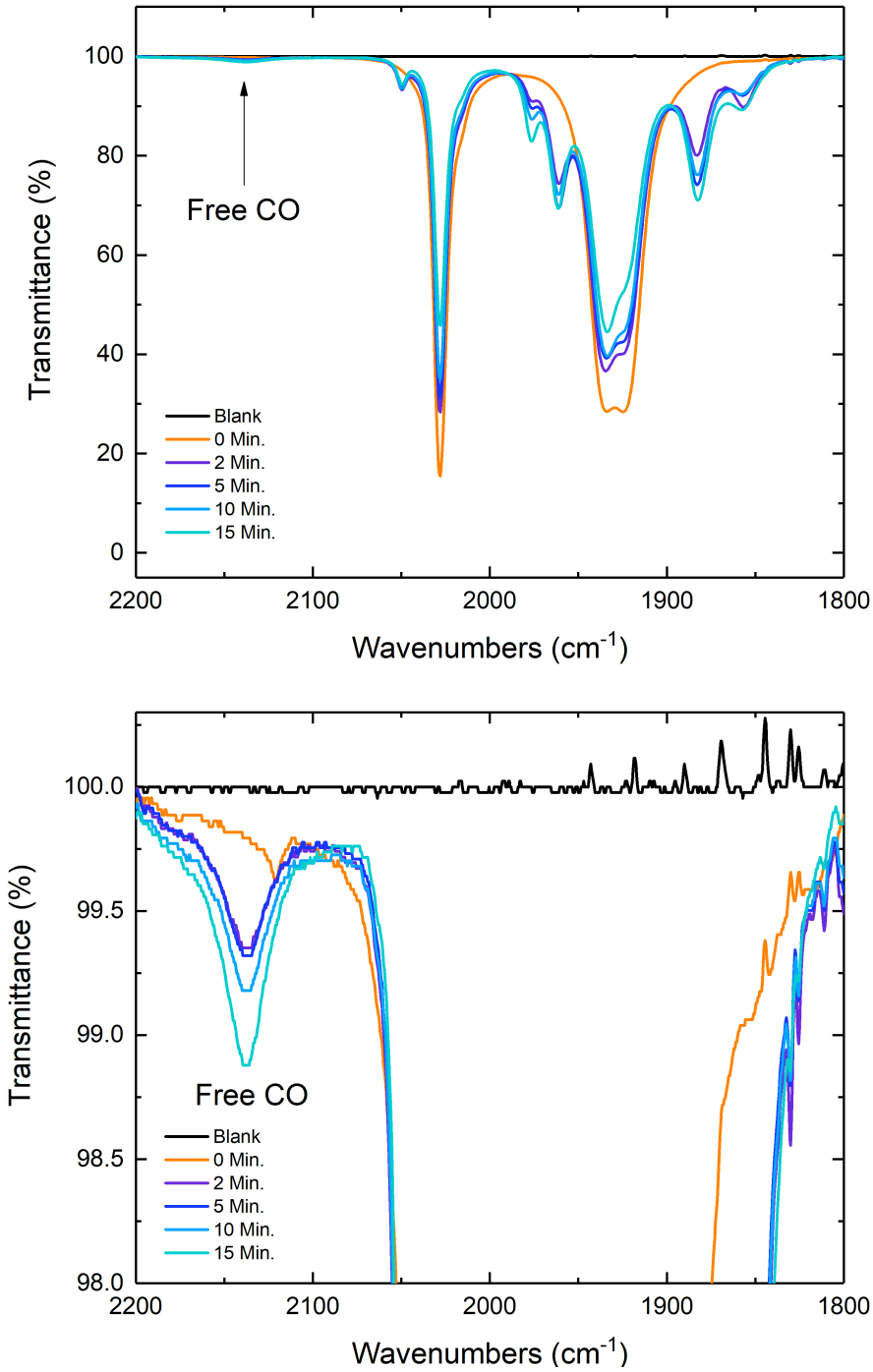

Figure S24: IR spectroscopic monitoring of a solution containing complex **2** irradiated over time with 415 nm light at 175 W. The irradiation results in follow-up chemical activity that is exhibited by the presence of new CO stretches in the IR spectrum after 2 min. of irradiation. The presence of free carbon monoxide is present after 2 min.

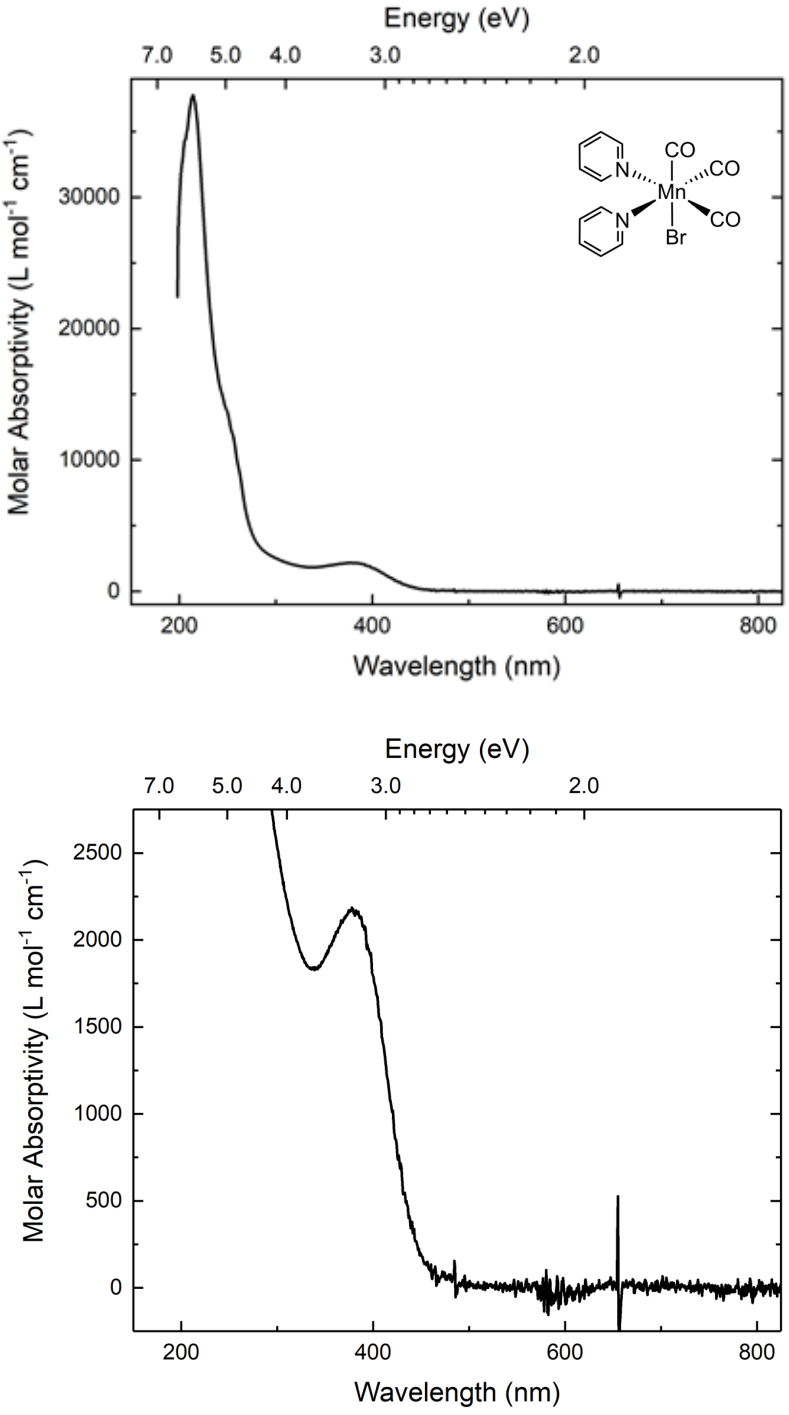

Figure S25: Electronic absorption spectrum of **5** in MeCN. The smaller tic marks are used to illustrate 0.1 eV increments.

Crystallographic Information

Refinement Details

Crystals were mounted on a nylon loop using Paratone oil under a nitrogen stream. Low temperature (200-296 K) X-ray data were obtained with a Bruker MicroStar microfocus rotating anode generator running at 50-60 mA and 45 kV (Cu Kα = 1.54178 Å; Apex II detector positioned at 50.0 mm and equipped with Helios multilayer mirror optics (Complexes **3** and **4**), or with a Bruker generator using a fine focus Mo sealed tube running at 30mA and 50kV (Mo Kα = 0.71073 Å; SMART APEX detector positioned at 50.0 mm and equipped with a MonoCap collimator and graphite monochromator (complex **5**). All diffractometer manipulations, including data collection, integration and scaling were carried out using the Bruker APEXII software.[1] Absorption corrections were applied using SADABS.[2] The space group was determined on the basis of systematic absences and intensity statistics and the structures were solved by intrinsic phasing using XT.[3] All non-hydrogen atoms were refined using anisotropic displacement parameters. Hydrogen atoms were placed in idealized positions and refined using a riding model. The structures was refined (weighted least squares refinement on F^2) to convergence using the Olex software package equipped with XL.[4]

Table S1: Crystal and Refinement Data

Compound	**3**	**4**	**5**
CCDC accession code	1922041	1922042	1922040
empirical formula	$C_{15}H_6BrF_6MnN_2O_3$	$C_{13}H_6N_4O_7MnBr$	$C_{13}H_{10}BrMnN_2O_3$
formula wt	510.07	465.07	377.08
T (K)	200	200	200
a, Å	19.666(2)	15.4742(7)	7.4387(17)
b, Å	10.4825(12)	9.8701(4)	14.408(3)
c, Å	17.0392(18)	21.8544(8)	13.148(3)
α, deg	90	90	90
β, deg	96.515(4)	107.363(3)	90.352(3)
γ, deg	90	90	90
V, $Å^3$	3489.9(7)	3185.8(2)	1409.1(6)
Z	8	8	4
cryst. syst	monoclinic	monoclinic	monoclinic
space group	C2/c	$P2_1/c$	Cc
ρ_{calcd}, g/cm^3	1.942	1.939	1.777
2θ range, deg	9.052 to 139.886	5.984 to 140.072	2.827 to 26.914
μ, mm^{-1}	9.594	10.143	3.779
abs corr	Multi-scan	Multi-scan	Multi-scan
GOOF[c]	1.042	1.052	1.014
R1,[a] wR2[b] (I > 2σ(I))	0.0654, 0.1734	0.0583, 0.1507	0.0277, 0.0602

[a] $R1 = \Sigma||F_o|-|F_c|| / \Sigma|F_o|$ [b] $wR2 = [\ \Sigma\ [w(F_o^2-F_c^2)^2] / \Sigma\ [w(F_o^2)^2]\ ]^{1/2}$ [c] $GOOF = S = [\ \Sigma\ [w(F_o^2-F_c^2)^2] / (n-p)\ ]^{1/2}$

Special Refinement Details for 5.

Diffraction data [6683 reflections using 1°-wide ω-scan frames with a scan time of 5 seconds] were collected[5] for a pseudomerohedrally-twinned crystal of **5** using graphite-monochromated MoKα radiation (λ= 0.71073 Å) on a Bruker SMART APEX CCD Single Crystal Diffraction System at 200 K. X-rays were provided by a fine-focus sealed X-ray tube operated at 50kV and 35mA. Lattice constants were determined with the Bruker SAINT software package using peak centers for 3524 reflections. The integrated data[6] were corrected empirically for variable absorption effects using equivalent reflections. The Bruker software package SHELXTL was used to solve the structure using "direct methods" techniques. All stages of weighted full-matrix least-squares refinement were conducted using F_o^2 data with the SHELXTL XL v2014 software package.[7] The final structural model incorporated anisotropic thermal parameters for all nonhydrogen atoms and isotropic thermal parameter for all hydrogen atoms. The pyridine hydrogen atoms were included in the structural model as idealized riding model atoms (assuming sp^2-hybridization of the carbon atoms and C-H bond lengths of 0.95 Å) and their isotropic thermal parameters were fixed at values 1.2 times the equivalent isotropic thermal parameter of the carbon atom to which they are covalently bonded. Final crystallographic details are summarized in Table S1.

Several aspects of the structure complicated its successful refinement. The similar size of a Br atom and a carbonyl ligand bonded to a Mn atom produced 83/17 "whole molecule" packing disorder of **5**. The major orientation is occupied 83% of the time and the minor is occupied 17% of the time. The structure is also pseudo-centrosymmetric: the fractional coordinates for the Mn atom coincide with those of a crystallographic C_2-axis in the centrosymmetric counterpart (C2/c) of the noncentrosymmetric space group (Cc) utilized by **5**. Additionally, the coordinated pyridine ligands and two of the carbonyls are also related by this pseudo-C_2 axis. Finally, a monoclinic β angle of 90.35° promotes 93/7 pseudo-merohedral (orthorhombic) twinning with the major (93%) domain also being 85/15 racemically twinned.

It is therefore not surprising that restraints had to be imposed in order to obtain a reasonable refinement. Bond lengths and angles for the minor (17%) orientation of **5** were restrained to be similar to those of the major (83%) orientation. The anisotropic thermal parameters for the nonhydrogen atoms (except O1′) of the minor orientation of **5** were set to the same values as the corresponding atoms of the major orientation. O1′ was assigned its own anisotropic thermal parameter that was allowed to vary. Other mild restraints were needed for the minor orientation of **5** to ensure linear carbonyl coordination and planar pyridine ligands.

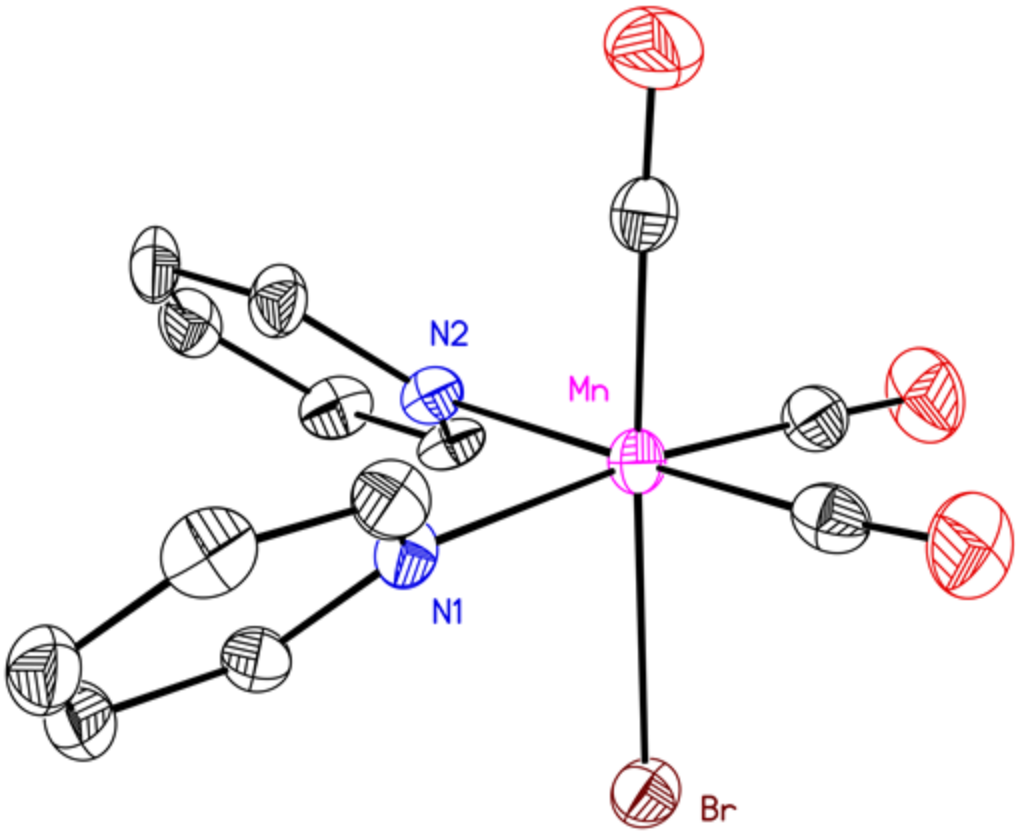

Figure S26: Solid-state structure of **5**. Hydrogen atoms and second molecule of **5** are omitted for clarity. Displacement ellipsoids shown at the 50% probability level.

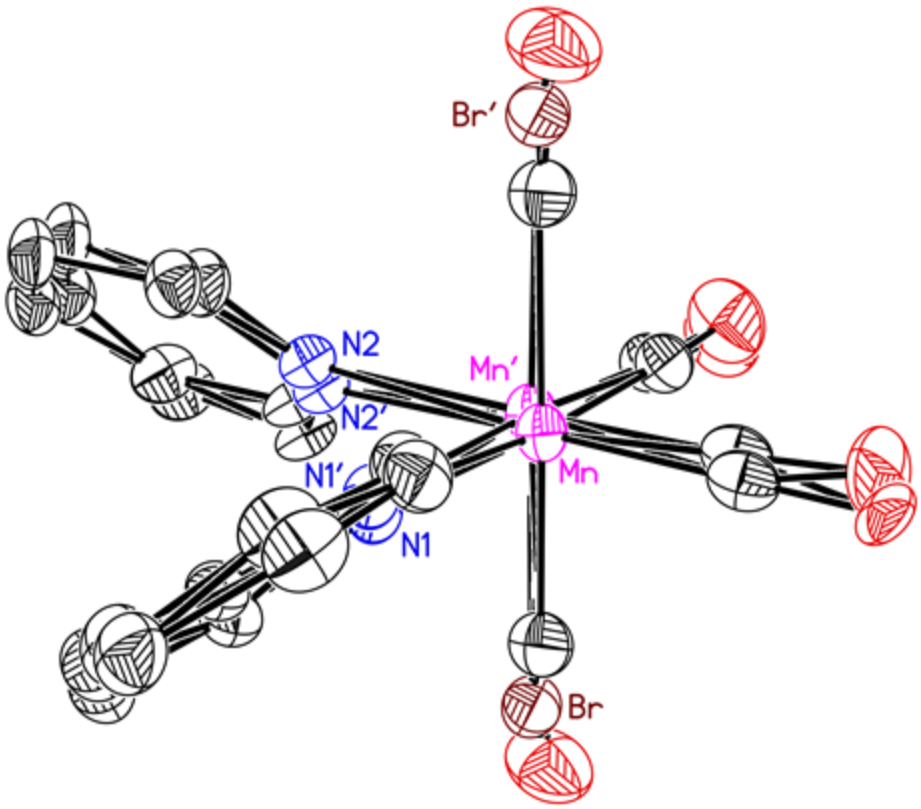

Figure S27: Full solid-state structure of **5**. Hydrogen atoms omitted for clarity. Displacement ellipsoids shown at the 50% probability level.

Special Refinement Details for 3.

No special refinement was required.

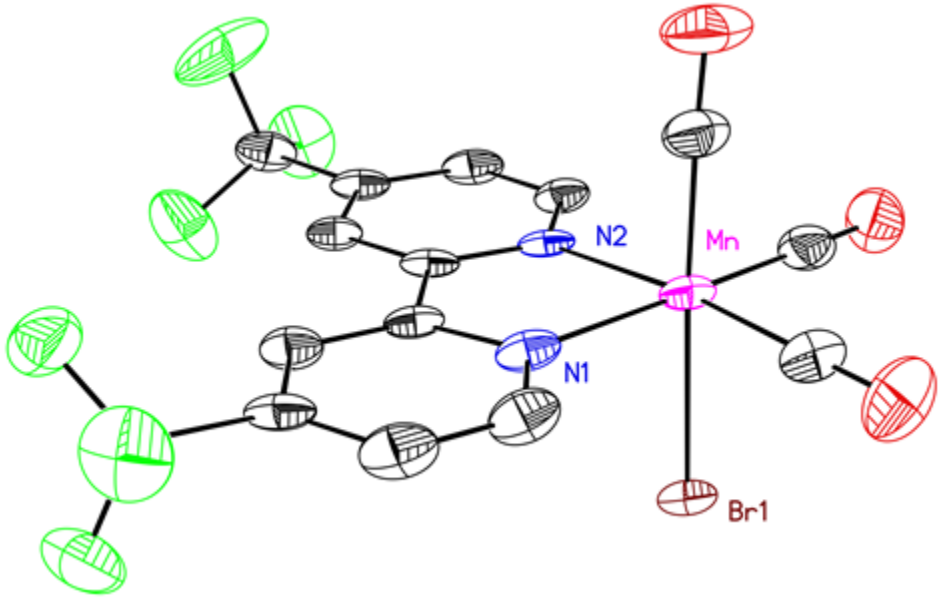

Figure S28: Full solid-state structure of **3**. Hydrogen atoms are omitted for clarity. Displacement ellipsoids shown at the 50% probability level.

Special Refinement Details for 4.

No special refinement was required.

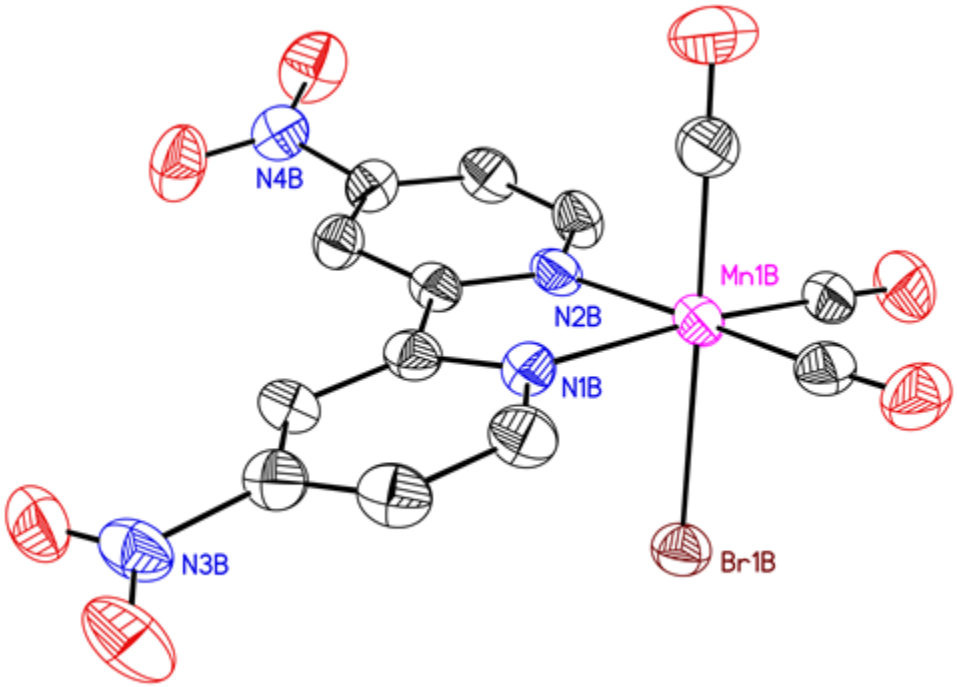

Figure S29: Solid-state structure of **4**. Hydrogen atoms and second molecule of **4** are omitted for clarity. Displacement ellipsoids shown at the 50% probability level.

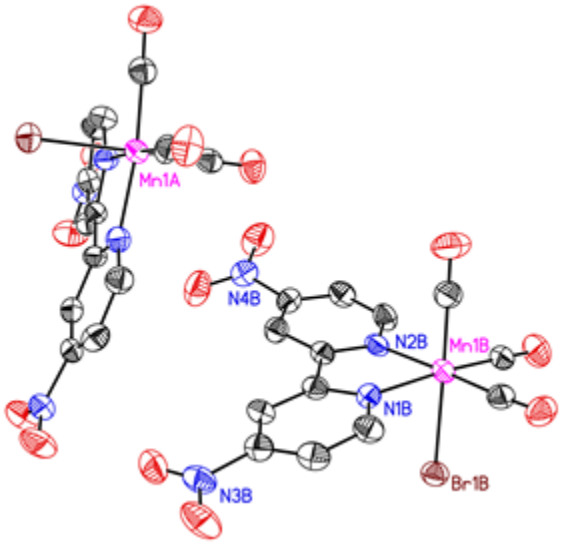

Figure S30: Full solid-state structure of **4**. Hydrogen atoms omitted for clarity. Displacement ellipsoids shown at the 50% probability level.

References

[1] *APEX2, Version 2 User Manual, M86-E01078,*; Bruker Analytical X-ray Systems: Madison, WI, June 2006.

[2] Sheldrick, G. M., SADABS (version 2008/1): Program for Absorption Correction for Data from Area Detector Frames, University of Göttingen, 2008.

[3] Sheldrick, G. Crystal structure refinement with SHELXL. *Acta Crystallogr., Sect. A: Found. Crystallogr.* **2015**, *71*, 3-8.

[4] Dolomanov, O. V.; Bourhis, L. J.; Gildea, R. J.; Howard, J. A. K.; Puschmann, H., *OLEX2*: A Complete Structure Solution, Refinement and Analysis Program, *J. Appl. Crystallogr.* **2009**, *42*, 339-341.

[5] Data Collection: SMART Software in APEX2 v2014.11-0 Suite. Bruker-AXS, 5465 E. Cheryl Parkway, Madison, WI 53711-5373 USA.

[6] Data Reduction: SAINT Software in APEX2 v2014.11-0 Suite. Bruker-AXS, 5465 E. Cheryl Parkway, Madison, WI 53711-5373 USA.

[7] Refinement: SHELXTL Software in APEX2 v2014.11-0 Suite. Bruker-AXS, 5465 E. Cheryl